Synthesis and characterization of MoOI2(PMe3)3, and use of MoOX2(PMe3)3 (X = Cl, I) in controlled radical polymerization

José A Mata, Sébastien Maria, Jean-Claude Daran, Rinaldo Poli

Synthesis and characterization of $MoOI_2(PMe_3)_3$, and use of $MoOX_2(PMe_3)_3$ (X = Cl, I) in controlled radical polymerization

José A. Mata, Sébastien Maria, Jean-Claude Daran and Rinaldo Poli*

Laboratoire de Chimie de Coordination, UPR CNRS 8241 lié par convention à l'Université Paul Sabatier et à l'Institut National Polytechnique de Toulouse, 205 Route de Narbonne, 31077 Toulouse Cedex, France.

Proofs to:

Rinaldo Poli

Tel: +33-561333195

Fax: +33-561553003

E-mail: **poli@lcc-toulouse.fr**

Keywords

Molybdenum, oxo ligands, phosphine ligands, halide exchange, atom transfer radical polymerization

Abstract

Complex $MoOCl_2(PMe_3)_3$ smoothly reacts with NaI in acetone to produce $MoOI_2(PMe_3)_3$ in good yields. The geometry of the compound is *mer*,*cis* octahedral, *i.e.* identical to that of the dichloride precursor, as shown by NMR spectroscopy and by an X-ray crystallographic study. Electrochemical investigations of $MoOX_2(PMe_3)_3$ show irreversible oxidation waves at $E_{p,a}$ = +0.18 and +0.39 V for X = Cl and I, respectively. A study of the halide exchange between $MoOCl_2(PMe_3)_3$ and NaI, or between $MoOI_2(PMe_3)_3$ and Bu_4NCl, shows two equilibrated isomers for the mixed halide intermediate $MoOICl(PMe_3)_3$. The diiodide complex exchanges rapidly the iodide ligands with chlorides upon dissolution in chloroform at room temperature, and with bromide from 1-phenyl-1-bromoethane (BEB) under more forcing conditions. The equilibrium favors the softer halide (I) on carbon and the harder one (Cl or Br) on Mo^{IV}. Both oxo compounds catalyze the atom transfer radical polymerization (ATRP) of styrene in combination with the BEB initiator, yielding polymers with quite narrow molecular weight distributions (down to 1.11). The apparent polymerization rate constant is ca. doubled in the presence of 1 equivalent of the $Al(O\textit{i}Pr)_3$ cocatalyst. On the other hand, the system is not capable to efficiently control the radical chain growth for methyl acrylate polymerization.

Introduction

In recent years, a number of coordination and organometallic compounds based on different transition metals have been proven capable to control the radical polymerization of activated olefins. The phenomenon is accomplished by maintaining the active radical concentration at very low levels though a fast reversible equilibrium with a dormant species, thereby reducing the incidence of bimolecular terminations. The equilibrium may implicate a halogen atom transfer (see Scheme 1), thus the term Atom Transfer Radical Polymerization (ATRP).[1, 2] In this respect, the process corresponds to a transition metal catalyzed multiple insertion of olefins into the carbon-halogen bond of the initiator molecule. A metal complex, however, may also yield a dormant species by reversibly forming a metal-carbon bond (see Scheme 2). This process is termed, somewhat inappropriately, Stable Free Radical Polymerization (SFRP). Indeed, the stable transition metal complex acting as a spin trap need not possess a radical character. We have recently proposed a new term for this process, Organometallic Radical Polymerization (OMRP), because it involves the reversible formation of a metal-carbon bond.[3]

<Scheme 1 and Scheme 2>

The various metals so far shown to be effective include Ti^{III},[4] Mo^{III},[5, 6] Re^{V},[7] Fe^{II},[8, 9] Ru^{II},[10] Ni^{II},[11] Ni^{0},[12] and Cu^{I}.[13] Although no system currently appears to parallel the activities and practical advantages of certain Cu^{I} complexes, the investigation of other metal systems is useful in order to shine additional light on the mechanistic details of the process. For instance, by using $CpMoCl_2L_2$ complexes (L = tertiary

phosphines or L_2 = diene), we have demonstrated how the two trapping processes in Scheme 1 and Scheme 2 may simultaneously take place when the polymerization is carried out under ATRP conditions.[5] Furthermore, the use of $MoX_3(PMe_3)_3$ catalysts (X = Cl, Br, I) has revealed that the oxidized metal complex (ATRP spin trap) need not be a thermodynamically stable species in order for the catalyst to ensure a good control.[14] In fact, whereas the Mo^{IV} complexes $MoX_3Y(PMe_3)_3$ (X, Y = Cl, Br) could be isolated and fully characterized, no such complex containing an iodide ligand was shown to exist, because it would decompose by an internal redox process to a Mo(III) complex and I_2. As a further example, a comparison of the rates of halide exchange between various ATRP catalysts [*i.e.* $MoX_3(PMe_3)_3$, $CpMoCl_2(RN{=}CHCH{=}NR)$ (R = *i*Pr), $RuCl_2(PPh_3)_3$] and initiator molecules, in the presence and in the absence of $Al(O\textit{i}Pr)_3$, has revealed two possible mechanisms for this exchange process.[15, 16]

The results of DFT calculations have shown that the Mo-X and Mo-R bond strengths decrease upon raising the metal oxidation state, the computed values suggesting that the $Mo^{III/IV}$ redox couple is ideally placed to insure appropriate equilibrium positions for both ATRP and SFRP processes. Indeed, complex $CpMo(CH_2SiMe_3)_2(\eta^4\text{-}C_4H_6)$ does not yield radical polymerization, showing that this particular Mo^{III}-R bond is too strong.[5] On the other hand, preliminary evidence, which will be reported separately, has indicated the possible implication of $Mo^{IV/V}$ couples in ATRP. For this reason, we have decided to test some typical Mo(IV) coordination compounds as ATRP catalysts. In this paper, we report our results obtained by using a well known Mo(IV) coordination compound, $MoOCl_2(PMe_3)_3$. In addition, we also report the results obtained with the related compound $MoOI_2(PMe_3)_3$, whose synthesis and characterization is reported here for the first time. Our interest in this compound was twofold. From the point of view of ATRP catalysis, we have shown that some iodo derivatives of certain Mo(III) ATRP catalysts,

e.g. $CpMoI_2(RN{=}CHCH{=}NR)$ (R = *i*Pr) are more active than the corresponding chloro derivatives.[15] From the coordination chemistry point of view, we have demonstrated the incompatibility between iodo ligands and Mo(IV) in complexes of type $MoX_nY_{4-n}(PMe_3)_3$ (*vide supra*).[14] Yet, stable iodide derivatives of molybdenum in higher oxidation states do exist when the metal electronic deficiency is satisfied by strongly donor ligands (*e.g.* $Cp^*Mo^{IV}I_4^-$ and $Mo^{V}OI_4^-$).[17, 18] Therefore, it was of interest to see whether compound $MoOI_2(PMe_3)_3$ would be stable, to investigate its redox properties, and to test its catalytic properties in ATRP.

Results and Discussion

(a) Syntheses and characterization

The new complex $MoOI_2(PMe_3)_3$ was obtained by halide exchange from the dichloride precursor as described in Scheme 3. The reaction is driven by the precipitation of the less soluble NaCl and is relatively rapid at room temperature. The spectroscopic properties of the isolated compound indicate an identical structure to that of the precursor. In particular, the ^{31}P NMR spectrum shows two types of phosphine ligands in a 2:1 ratio, whereas the virtual triplet pattern for the ^{1}H NMR resonance of the two equivalent PMe_3 ligands establishes their mutual *trans* arrangement (the spectral parameters are collected in Table 1). This clearly identifies the *mer* arrangement of the $Mo(PMe_3)_3$ moiety. The ^{31}P NMR spectrum is qualitatively different in acetone-d_6 and in C_6D_6. Whereas the doublet-triplet pattern expected for an AX_2 spin system is relatively unperturbed in the former solvent, a more complex pattern, which is indicative of second order coupling for an AB_2 system, is evident in C_6D_6, see Figure 1. This

difference is caused by the closer proximity of the two ^{31}P resonances in C_6D_6. The values reported in Table 1 result from the successful simulation of the spectrum.

<Figure 1>

The relative *cis* arrangement of the two iodide ligands is unambiguously confirmed by the single crystal X-ray diffraction study, but is also indicated by the NMR monitoring of the halide exchange process, notably by the presence of *two* different stereoisomers for the mixed halide complex *(vide infra).* When using a sufficiently large excess of NaI (> 5 equiv), the isolated product is devoid of any mixed halide impurity. It is also devoid of the known[19] Mo^{III} complex $MoI_3(PMe_3)_3$, a problem that often affects its dichloride precursor $MoOCl_2(PMe_3)_3$.[20] Indeed, the latter is usually obtained from $MoCl_4(THF)_2$ and PMe_3 in the presence of water,[21] giving a product whose color (varying from blue to green) depends on the level of contamination by yellow $MoCl_3(PMe_3)_3$. By replacing the tetrachloride Mo^{IV} precursor with the bis(ether) complex, $MoCl_4(Et_2O)_2$,[22] we have obtained a blue material that is also contaminated by minor amounts of the trichloride Mo^{III} complex, as evidence by ^1H NMR. A better synthesis of pure $MoOCl_2(PMe_3)_3$ is that reported by Galindo *et al.*, from $MoO_2Cl_2(MeOCH_2CH_2OMe)$ and PMe_3.[23] Our synthesis of $MoOI_2(PMe_3)_3$ was carried out from a dichloride precursor obtained by the latter procedure.

<Scheme 3 and Table 1>

A view of the molecule resulting from the X-ray diffraction study is shown in Figure 2. The relevant geometric parameters are collected in Table 2. The thermal

ellipsoids are well behaved, showing no evidence for positional disorder, in agreement with the NMR evidence for the absence of $MoI_3(PMe_3)_3$. In addition, the presence of iodide in the oxo position would have a notable effect on the refined Mo=O distance, whereas the experimental value of 1.685(4) Å is quite short. Moreover, this distance is identical within experimental error to the distance reported for the corresponding complex *cis-mer*-$MoOCl_2(PMe_2Ph)_3$ [1.675(3) Å].[20] Therefore, these results show that there is no compositional I, O disorder, contrary to previous reports for the dichloro analogues.[20] The Mo-P distances [2.494-2.513 Å] are within the normal range for related compounds.

<Figure 2 and Table 2>

From a benzene/*n*-pentane solution of $MoOCl_2(PMe_3)_3$ set aside for several days, crystals of compound $[MoOCl(PMe_3)(OPMe_3)]_2(\mu\text{-}O)$ were obtained, possibly by adventitious contact with air and moisture. Since the resulting structure is more accurately determined and is in a different crystal system than one reported previously for the same compound,[24] we report it here but do not comment on it any further. No analogous compound was obtained from the corresponding oxo diiodide complex.

The existence and stability of the $MoOI_2(PMe_3)_3$ compound [*cf.* the non existence of $MoI_4(PMe_3)_3$][14] indicates that the oxo ligand is a much stronger electron donor than two iodide ligands toward the Mo center, raising the energy of the LUMO and thereby making the metal center a less powerful oxidizing agent. Indeed, qualitative MO considerations lead to the expectation of an interaction as shown in Scheme 4, where the energy of the d_{xz} and d_{yz} orbitals of the pseudo-t_{2g} set (octahedral coordination environment) is raised through the π-donation mechanism.

<Scheme 4>

An electrochemical investigation of compounds $MoOX_2(PMe_3)_3$ yields irreversible oxidation processes at $E_{p,a}$ = +0.18 and +0.39 V for X = Cl and I, respectively, see Figure 3. The lack of reversibility indicates the occurrence of a fast chemical process after oxidation to the cationic Mo^V complex $[MoOX_2(PMe_3)_3]^+$, probably involving solvent coordination. The voltammogram recorded on the chloride complex shows that a new and broad cathodic peak is generated after the oxidation peak (this feature is not observed during the first cathodic scan prior to the oxidation peak). In the presence of chloride ions, the oxidation peak shifted slightly toward less positive potentials, but the overall shape of the voltammogram was otherwise unaffected. This result can be rationalized by a follow-up coordination of Cl^- to $[MoOCl_2(PMe_3)_3]^+$, with generation of the putative ATRP spin trap, $MoOCl_3(PMe_3)_3$. The same phenomenon was previously observed by us for the oxidation of $MoX_3(PMe_3)_3$ in the presence of X^- (X = Cl, Br) and verified by an independent study of the isolated $MoX_4(PMe_3)_3$ products.[14] In the present case, a similar verification is impossible because, to the best of our knowledge, complex $MoOCl_3(PMe_3)_3$ is non existent. Indeed, the voltammetric response in the presence of Cl^- shows that such compound is unstable under the condition of the CV experiment (THF solution) and decomposes in a similar way to that of the $[MoOCl_2(PMe_3)_3]^+$ complex.

<Figure 3>

Concerning the voltammogram of the diiodide complex, the greater oxidation potential relative to the dichloride analogue parallels the corresponding shift for the Mo^{III} complexes $MoX_3(PMe_3)_3$ upon going from X = Cl to I.[14] Note the presence of a small reversible wave at ca. -0.1 V in this voltammogram. This corresponds to the oxidation of I^- to I_3^- (as verified by the deliberate addition of I^- to the solution) and grows with the time lapse between the solution preparation and the voltammetric study. Even upon rapidly recording the voltammogram (as in the example shown in Figure 3), this feature could not be completely eliminated, suggesting the establishment of a slow ligand substitution equilibrium between iodide and THF. The other important observation is that the oxidation of I^- occurs at a less positive potential relative to the oxidation of the Mo^{IV} oxo complex. This has implications for the ATRP process (*vide infra*).

It is interesting to compare the oxidation potentials of $MoOX_2(PMe_3)_3$ with those of the corresponding $MoX_4(PMe_3)_3$. Because of its non-existence, the $E_{1/2}$ for the oxidation of $MoI_4(PMe_3)_3$ could not be established, but those of the analogous $MoX_4(PMe_3)_3$ complexes are -0.15 V (X = Cl) and -0.06 V (X = Br), allowing to extrapolate a value of ca. +0.05 for X = I. Thus, we can observe that the replacement of two X ligands by one O ligand has the effect of raising the oxidation potential by ca. 0.3 V. This change can be related to a lower energy of the HOMO for the oxo compound (Scheme 4), resulting from the greater electronegativity of the oxygen atom. In other words, there is less electron donation by one O relative to two I atoms via the σ bonding mechanism.

(b) NMR study of the halide exchange reactions

The conversion of the dichloride to the diiodide complex was followed by ^1H and ^{31}P NMR in the presence of NaI in acetone-d_6. Figure 4 shows representative $^{31}P\{^1H\}$

NMR spectra recorded during the transformation. The resonance values for the different compounds are collected in Table 1. Given the *mer-cis* coordination, there are two possible stereoisomers for the mixed-halide intermediate, **A** and **B** (see Scheme 5). A *mer-trans* or a *fac* arrangement would only allow a single stereoisomer. The monitoring clearly shows the preferential formation of isomer **A**. The structural assignment of **A** and **B** as shown in Scheme 5 is strongly suggested by the δ_P resonance pattern, especially the chemical shift of the unique P nucleus, which is expected to be most sensitive to the nature of the *trans* halide ligand. This resonance shifts very little during the first substitution for isomer **A**, whereas it shifts by a large amount for isomer **B**, to a position close to that observed for the final product. The two mutually *trans* P nuclei (*cis* to both halide coordination positions), on the other hand, shift gradually with the halide substitution.

<Figure 4 and Scheme 5>

A preferential formation of **A** would seem consistent with a kinetic control of the halide exchange, since the oxo ligand should exert a stronger *trans* effect relative to the PMe_3 ligand. However, the conversion in the opposite direction, which occurs in the presence of $Bu_4N^+Cl^-$ in acetone-d_6, yields again isomer **A** as the *major* intermediate. If the exchange process had been under kinetic control, the prevalence of isomer **B** was expected. Therefore, we conclude that the halide exchange process is under thermodynamic control and that the position *trans* to the oxo ligand is preferentially occupied by the softer iodide ligand.

In order to gain further insight on this issue, we have also carried out a reaction between $MoOI_2(PMe_3)_3$ and NaBr in acetone-d^6. The reaction qualitatively follows the

same pathway (see Scheme 6). The use of a small excess amount of NaBr (ca. 1.3 equiv) leads to rapid equilibration (4 h at room temperature) with the two mixed halide intermediates having structures **A'** and **B'**, the former being predominant, plus a small amounts of the corresponding dibromide. Treatment with an excess of NaBr increases the amount of dibromide product. The ^{31}P resonance of the unique PMe_3 ligand shifts from δ -12.5 from the diodide complex to δ -3.6 to **A'** and only to δ -10.3 for **B'**. The same nucleus resonates at δ -2.8 for the dibromide complex. Once again, the trans position to the oxo ligand shows a thermodynamic preference for the softer iodo ligand.

<Scheme 6>

It is interesting to note that complex $MoOI_2(PMe_3)_3$ rapidly yields halide exchange when dissolved in chloroform (ca. 50% in 30 min at room temperature). The NMR monitoring indicates the intermediate formation of the mixed halide isomers **A** (major) and **B** (very minor), though the exchange is eventually complete. In dichloromethane, this exchange is much slower, since no significant amount of mixed halide species (**A**) is formed after 20 h stirring at room temperature. This phenomenon could either take place by an internal nucleophilic substitution assisted by solvent coordination to the metal center, as we have recently pointed out for other transition metal complexes,[16] or by reversible atom transfer. In the latter case, the phenomenon would suggest that this system could serve as a good catalyst in atom transfer radical polymerization. This has indeed been verified experimentally (*vide infra*).

Since $MoOI_2(PMe_3)_3$ rapidly exchanges its halogen atoms with chloroform, we have also tested the halogen exchange with the initiator molecule used in ATRP, namely 1-bromethylbenzene, $PhCH(Br)CH_3$ (BEB). The reaction (Scheme 7) was followed by

^{1}H NMR, since the methyne proton is very sensitive to the nature of the halogen atom. At 90°C in toluene-d_8 and using a stoichiometric BEB/Mo ratio (same conditions used for the ATRP experiments, *vide infra*), the exchange process is essentially complete in 40 minutes, see Figure 5. A slower exchange is also observed at room temperature. ^{31}P NMR monitoring shows that the reaction proceeds through the same intermediates seen when using NaBr, namely $MoOBrI(PMe_3)_3$ (**A'** and **B'**, the former being predominant). The quantitative nature of the exchange illustrates the thermodynamic preference for placing the heavier halogen on the carbon atom and the lighter one on the metal. On the basis of Pearson's HSAB theory,[25] this result may be interpreted in terms of a harder character for the Mo^{IV} center with respect to carbon.

<Scheme 7 and Figure 5>

(c) Controlled Radical Polymerizations

Complexes $MoOX_2(PMe_3)_3$ were tested as catalysts for the controlled radical polymerization of styrene and methyl acrylate under ATRP conditions. The experimental conditions and apparent polymerization rates for the styrene polymerization are summarized in Table 3. In each case, the first order monomer consumption rate was verified by the linearity of the $\ln([M]_0/[M])$ *vs.* time plot, indicating that the concentration of active radical remains constant throughout the polymerization process, as expected for a controlled process. The polymerization was carried out both in the absence and in the presence of an equivalent amount of the $Al(O\textit{i}Pr)_3$ cocatalyst, whose effectiveness in ATRP seems quite general. In fact, it has been demonstrated that the apparent polymerization rates increase by factors up to 10 or more when one equivalent of this compound is used in conjunction with a variety of different catalysts based on Group 6-

11 metals, including $CpMoCl_2$(*i*PrN=CH-CH=N*i*Pr),[6] $MoX_3(PMe_3)_3$,[14] $ReIO_2(PPh_3)_2$,[7] $CpFeX(CO)_2$ (X = Br, I),[8] $RuCl_2(PPh_3)_3$,[10] $NiBr_2(PPh_3)_2$,[11] $Ni(PPh_3)_4$,[12] and CuBr/bipy.[13] The proposed mode of action of this cocatalyst consists of a shift of the atom transfer equilibrium, caused by the stronger interaction of the Al Lewis acid with the halogen lone pairs in the more polarized Mo-X bond, relative to the C-X bond of the initiator/dormant species.[16] Table 3 shows that $Al(OiPr)_3$ is also effective in conjunction with the $MoOX_2(PMe_3)_3$ catalysts, although by a smaller margin. In each case, the apparent polymerization rate approximately doubles when one equivalent of $Al(OiPr)_3$ is added. Note also that the diiodide system is about twice as fast as the dichloride system.

<Table 3>

For each dihalide catalyst and in the absence of $Al(OiPr)_3$, the experimentally determined number-average molecular weights (M_n) of the polymer grows linearly with the monomer conversion and corresponds closely to the theoretical molecular weights on the basis of the monomer/initiator ratio, see Figure 6 (*a* and *c*). These characteristics are as expected for a controlled radical polymerization process. Furthermore, the polydispersity indexes (PDI = $\overline{M_w}/\overline{M_n}$) are quite low, down to 1.11. These are the lowest PDI's reported to date for a Mo-based catalyst, underlining the excellent level of control exerted by these oxomolybdenum(IV) complexes. At high conversions, the experimental M_n is slightly lower than the theory for the dichloride system, whereas it is slightly higher for the iodide system. The former effect could result from the slight intervention of chain transfer processes, whereas the latter one could find a rationalization in an initiator efficiency slightly lower than 100% ($f < 1$). In the presence of $Al(OiPr)_3$,

the dichloride catalyst appears to insure a less effective control, since the PDI's are higher (ca. 1.3 at 75% conversion), although M_n still grows linearly with conversion, see Figure 6(*b*), and the monomer consumption follows first order kinetics. In addition, the experimental M_n is ca. two times greater than the calculated value (*i.e.* f = ca. 0.5). The diiodide catalyst also controls the polymerization a little less effectively in the presence of $Al(OiPr)_3$, but f remains close to 1, see Figure 6(*d*). At the moment, we are not able to rationalize why the nature of the halogen has such a large effect on the initiator efficiency, and only for the experiments carried out in the presence of $Al(OiPr)_3$.

<Figure 6>

The putative coordination compounds produced by the atom transfer process could not be characterized. From the electrochemical study, we have established that the oxidation potentials of complex $MoOCl_2(PMe_3)_3$ is less positive that those of the free Cl^- or Br^- ions.[14] Therefore, the oxidized complex $[MoOCl_2(PMe_3)_3]^+$ is compatible with the presence of these ions or, in other words, complex $MoOCl_2X(PMe_3)_3$ (X = Cl, Br) is predicted to be a stable system from the redox point of view. Nonetheless, the electrochemical study indicates instability for $MoOCl_3(PMe_3)_3$, at least in the THF solvent used for the cyclic voltammetric investigation. On the other hand, the free iodide ion is oxidized at a less positive potential than both complexes $MoOX_2(PMe_3)_3$ (X = Cl, I). This means that the putative ATRP spin trap, namely a Mo^V oxo complex of type $MoOX_2Y(PMe_3)_3$, is thermodynamically unstable when either X or Y is an iodine atom, relative to an internal redox process leading to the reduction of Mo^V to Mo^{IV} and oxidation of I^-. This observation might seem inconsistent with the ability of $MoOI_2(PMe_3)_3$, in combination with a bromide initiator, to catalyze the ATRP of styrene

with a controlled chain growth. However, our recently published investigation of the $MoI_3(PMe_3)_3$ ATRP catalyst, for which the same apparent contradiction was observed, provides the basis to rationalize this phenomenon.[14] In essence, the oxidized $MoOI_2Br(PMe_3)_3$ complex is capable to efficiently act as a spin trap for the growing radical chain for kinetic reasons, its decomposition being a bimolecular reaction and involving a greater activation barrier than the radical trapping process.

The polymerization of methyl acrylate was not well controlled by these Mo^{IV} oxo complexes. Initial experiments carried out with each dihalide complex at 90° with ethyl 2-iodopropionate as an initiator gave very fast polymerizations, with greater than 90% conversion after the first 300 minutes. The reaction was therefore repeated at a lower temperature (35°C). Even under these conditions, however, the polymerization process remained quite fast. With complex $MoOCl_2(PMe_3)_3$ the conversion was initially high and slowed down at later times (the monomer decay did not follow a 1^{st} order rate law), reaching a ca. 60% conversion in 6 days. With complex $MoOI_2(PMe_3)_3$, the process was even faster, reaching 100% conversion in ca. 18 h. In both cases, the molecular weights were much greater than expected on the basis of a controlled process, and the PDI's were quite high (> 1.5), see for instance Figure 7 for the chloride system. This behavior is consistent with an atom transfer process that is not sufficiently shifted toward the dormant species. Further studies under different conditions (nature of the initiator, different co-catalysts) will need to be carried out in order to optimize this process.

<Figure 7>

In order to check whether the OMRP equilibrium also plays a role in the ATRP catalyzed by $MoOX_2(PMe_3)_3$, the polymerization of styrene was also carried out using AIBN as a thermal initiator in the presence of these compounds. After heating at 100°C

for 30 minutes to decompose most of the initiator, the temperature was set to 80°C for the rest of the experiment. The polymerizations were not controlled, with conversions reaching 30% within the first 4 h and then increasing slowly to 65% over the next 4 days. There was no first order monomer consumption, and the PDI's remained consistently high throughout the experiment. These results are typical of an uncontrolled free radical process. Only a minor retardation effect was noted in the presence of the metal complexes, *e.g.* see Figure 8. This suggest the possibility of a radical trapping process by the $MoOX_2(PMe_3)_3$ complex, but the stability of the adduct is insufficient. In conclusion, the $MoOX_2(PMe_3)_3$ complexes are not capable to efficiently trap the reactive radical of polystyrene and form sufficiently persistent dormant species.

<Figure 8>

Conclusions

The current investigation has shown, for the first time, the ability of Mo^{IV} complexes to function as ATRP catalysts. Both the well known dichloro complex and its newly developed diiodo analogue are equally capable to produce polystyrenes with rather narrow polydispersities. The diiodide catalyst gives higher apparent polymerization rates, and the rate is further doubled in the presence of one equivalent of $Al(O\textit{i}Pr)_3$ for each catalyst. We could not isolate and characterize the metallic spin traps, which are expected to be Mo^{V} complexes of formula $MoOX_2Y(PMe_3)_3$ (X, Y = Cl, Br, I). The electrochemical studies indicate instability for these complexes, at least in THF. In addition, the iodide-containing system is thermodynamically unstable with respect to an intramolecular redox process. However, as we have recently demonstrated for a related

catalyst,[14] it is not necessary for the spin trap to be a thermodynamically stable compound. It remains competent to perform the radical trapping function, thereby regulating the concentration of the active organic radical, for kinetic reasons. We are now interested in testing these oxomolybdenum(IV) complexes as well as other similar compounds in the polymerization (under ATRP and SFRP conditions) of other monomers.

Experimental Section

All the manipulations were carried out under an atmosphere of dry and oxygen-free argon with standard Schlenk techniques. Styrene was washed with an aqueous NaOH (10%), neutralized with water, dried over $MgSO_4$ and then distilled at 25ºC under reduced pressure. Toluene and pentane were purified by distillation under argon after drying over sodium benzophenone ketyl. CH_2Cl_2 was purified from P_4O_{10} and distilled under argon. 1-Phenyl-1-bromoethane (or 1-bromoethylbenzene, BEB) and $Al(OiPr)_3$ were purchased from Aldrich Chemical Co, and used as received. Complex $MoOCl_2(PMe_3)_3$ was prepared according to the literature.[21, 23] A slight modification of the procedure described in ref. [21], with use of complex $MoCl_4(EtO)_2$ instead of $MoCl_4(THF)_2$ as starting material, gave the product in the form of a blue solid containing a few % of the $MoCl_3(PMe_3)_3$ by-product, as shown by ^1H NMR.[20] The procedure described in ref. [23] afforded a pure product (deep blue solid) in 70% yields.

Physical Measurements. The cyclic voltammograms were obtained with an EG&G 362 potentiostat connected to a Macintosh computer through MacLab hardware/software. The electrochemical cell was fitted with a Ag-AgCl reference electrode, a platinum disk working electrode and a platinum wire counterelectrode.

$[Bu_4N]PF_6$ (ca. 0.1 M) was used as supporting electrolyte. The ferrocene standard was added to each solution and measured at the end of the experiments. Its potential is $E_{1/2}$ = +0.50 V under our experimental conditions. NMR spectra were recorded on a Bruker DRX 400 MHz spectrometer. The peaks positions are reported with positive shifts in ppm downfield of TMS, as calculated from residual solvent peaks. Digital simulation of the ^{31}P NMR spectrum was carried out with MestReC.[26] The molecular weight distribution, $\overline{M_n}$ and $\overline{M_w}/\overline{M_n}$ of the polymers were measured by size-exclusion chromatography (SEC) using THF as eluent (1mL/min) at room temperature on a 300x7,5 mm PLgel 5µm Mixed-D column (Polymer Laboratories), equipped with multiangle light scattering (miniDawn Tristar, Wyatt Technology Corp.) and refractive index (RI2000, Soparès) detectors.

Synthesis of $MoOI_2(PMe_3)_3$. To a solution of $MoOCl_2(PMe_3)_3$ (435mg, 1.06 mmol) in THF (15 mL) freshly distilled was added an excess of NaI (795 mg, 5.3 mmol). The solution was then stirred at 50 ºC for two hours to achieve completion although after ten minutes it is possible to observe the formation of a white precipitate of NaCl. After removing the volatiles under reduce pressure the crude was redissolved in toluene (15 mL) to eliminate the insoluble salts of NaI and NaCl. Then pentane (25 mL) was added to the toluene solution to precipitate complex $MoOI_2(PMe_3)_3$ as an emerald-green solid, which was filtered and washed twice with pentane (2 x 10mL). Yield 314 g, 50%. Single crystals for X-ray diffraction were obtained by slow diffusion of pentane into a concentrated solution of the product in toluene. The NMR properties are collected in table 1. Elemental analysis for $C_9H_{27}I_2MoOP_3$ (593.98): calcd. C, 18.20; H, 4.58; found C, 18.30; H, 4.28. The compound is soluble and stable in THF, acetone and aromatic hydrocarbons. It dissolves in $CDCl_3$ but gives rise to rapid halogen exchange in this solvent.

X-ray structural studies. A single crystal of each compound was mounted under inert perfluoropolyether on the tip of glass fibre and cooled in the cryostream of either the Stoe IPDS diffractometer [for $MoOI_2(PMe_3)_3$] or the Oxford-Diffraction XCALIBUR CCD diffractometer [for $\{MoCl_2O(PMe_3)(OPMe_3)\}_2O$]. The structures were solved by direct methods (SIR97)[27] and refined by least-squares procedures on F^2 using SHELXL-97.[28] All H atoms attached to carbon were introduced in idealised positions and treated as riding models. The absolute structure for $MoOI_2(PMe_3)_3$ was confirmed by the refinement of the Flack's enantiopole parameter[29, 30] and by careful examination of the sensitive reflexions. The drawing of the molecules was realised with the help of ORTEP32.[31] Crystal data and refinement parameters are shown in Table 4.

Crystallographic data (excluding structure factors) have been deposited with the Cambridge Crystallographic Data Centre as supplementary publication no. CCDC 294667 and 294668. Copies of the data can be obtained free of charge on application to the Director, CCDC, 12 Union Road, Cambridge CB2 1EZ, UK (fax: (+44) 1223-336-033; e-mail: deposit@ccdc.cam.ac.uk).

Controlled Radical Polymerizations. All ATRP polymerization reactions were conducted following the same experimental procedure. A typical procedure is described as a representative example. $MoOCl_2(PMe_3)_3$ (54 mg, 0,13 mmol) was added to a 25 mL Schlenk tube equipped with a stirring bar. Styrene (3 mL, 26 mmol), toluene (6 mL) and (1-bromoethyl)benzene (17,7 μL, 0.13 mmol) were added to the reaction flask by a syringe after a 20 min Ar purge. The Schlenk tube was immersed in an oil bath heated at 90°C. Aliquots were withdrawn periodically for monitoring.

All OMRP polymerization reactions were conducted following the same experimental procedure. A typical procedure is described as a representative example.

$MoOI_2(PMe_3)_3$ (21 mg, 0,035 mmol) and AIBN (2.9 mg, 0.018 mmol) were added to a 15 mL Schlenk tube equipped with a stirring bar. Styrene (1 mL, 8.7 mmol), and toluene (2 ml) were added to the reaction flask by a syringe after a 20 min Ar purge. The Schlenk tube was immersed during 30 min in an oil bath heated at 100°C and at 80°C for the remainder time of the reaction. Aliquots were withdrawn periodically for monitoring. The yield of polymer, and thus the % conversion, for each withdrawn aliquot was calculated by the mass ratio before and after the complete removal of solvent and residual monomer by evaporation, until achievement of constant weight.

Acknowledgements. We are grateful to the CNRS for support of this work and to Sandrine Vincendeau for technical assistance. JAM thanks the Ministerio de Educación y Ciencia of Spain for a post-doctoral fellowship. SM thanks the Conseil Régional de Bourgogne and the CNRS for a BDI fellowship.

References

[1] K. Matyjaszewski, J. H. Xia, *Chem. Rev.* **2001**, *101*, 2921-2990.

[2] M. Kamigaito, T. Ando, M. Sawamoto, *Chem. Rev.* **2001**, *101*, 3689-3745.

[3] R. Poli, *Angew. Chem. Int. Ed. Engl.* **in press**.

[4] Y. Kabachii, S. Kochev, L. Bronstein, I. Blagodatskikh, P. Valetsky, *Polym. Bull.* **2003**, *50*, 271-278.

[5] E. Le Grognec, J. Claverie, R. Poli, *J. Am. Chem. Soc.* **2001**, *123*, 9513-9524.

[6] F. Stoffelbach, D. M. Haddleton, R. Poli, *Eur. Polym. J.* **2003**, *39*, 2099-2105.

[7] Y. Kotani, M. Kamigaito, M. Sawamoto, *Macromolecules* **1999**, *32*, 2420-2424.

[8] Y. Kotani, M. Kamigaito, M. Sawamoto, *Macromolecules* **1999**, *32*, 6877-6880.

[9] V. C. Gibson, R. K. O'reilly, W. Reed, D. F. Wass, A. J. P. White, D. J. Williams, *Chem. Commun.* **2002**, 1850-1851.

[10] T. Ando, M. Kamigaito, M. Sawamoto, *Macromolecules* **2000**, *33*, 6732-6737.

[11] H. Uegaki, Y. Kotani, M. Kamigaito, M. Sawamoto, *Macromolecules* **1997**, *30*, 2249-2253.

[12] H. Uegaki, M. Kamigaito, M. Sawamoto, *J. Polym. Sci., Polym. Chem.* **1999**, *37*, 3003-3009.

[13] J. Guo, Z. Han, P. Wu, *J. Mol. Catal. A* **2000**, *159*, 77-83.

[14] S. Maria, F. Stoffelbach, J. Mata, J.-C. Daran, P. Richard, R. Poli, *J. Am. Chem Soc.* **2005**, *127*, 5946-5956.

[15] F. Stoffelbach, R. Poli, *Chem. Commun.* **2004**, 2666 - 2667.

[16] R. Poli, F. Stoffelbach, S. Maria, J. Mata, *Chem. Eur. J.* **2005**, *11*, 2537-2548.

[17] J. U. Desai, J. C. Gordon, H.-B. Kraatz, V. T. Lee, B. E. Owens-Waltermire, R. Poli, A. L. Rheingold, C. B. White, *Inorg. Chem.* **1994**, *33*, 3752-3769.

[18] J. C. Gordon, S. P. Mattamana, R. Poli, P. E. Fanwick, *Polyhedron* **1995**, *14*, 1339-1342.

[19] F. A. Cotton, R. Poli, *Inorg. Chem.* **1987**, *26*, 1514-1518.

[20] K. Yoon, G. Parkin, A. L. Rheingold, *J. Am. Chem. Soc.* **1991**, *113*, 1437-1438.

[21] E. Carmona, A. Galindo, L. Sanchez, A. J. Nielson, G. Wilkinson, *Polyhedron* **1984**, *3*, 347-352.

[22] F. Stoffelbach, D. Saurenz, R. Poli, *Eur. J. Inorg. Chem.* **2001**, 2699-2703.

[23] T. Robin, F. Montilla, A. Galindo, C. Ruiz, J. Hartmann, *Polyhedron* **1999**, *18*, 1485-1490.

[24] F. A. Cotton, L. M. Daniels, S. Herrero, *Acta Cryst., C* **1999**, *C55*, IUC9900018.

[25] J. E. Huheey, E. A. Keiter, R. L. Keiter, *Inorganic Chemistry. Principles of Structure and Reactivity*, 4th ed., Harper & Row, New York, **1993**.

[26] *MestReC, v. 446*, Mestrelab Research, Santiago de Compostela, Spain, **2005**.

[27] A. Altomare, M. Burla, M. Camalli, G. Cascarano, C. Giacovazzo, A. Guagliardi, A. Moliterni, G. Polidori, R. Spagna, *J. Appl. Cryst.* **1999**, *32*, 115-119.

[28] G. M. Sheldrick, *SHELXL97. Program for Crystal Structure refinement*, University of Göttingen, Göttingen, Germany, **1997**.

[29] H. D. Flack, Acta Cryst. **1983**, *A39*, 876-881.

[30] G. Bernardinelli, H. D. Flack, *Acta Cryst., Sect A* **1985**, *41*, 500-511.

[31] L. J. Farrugia, *J. Appl. Crystallogr.* **1997**, *32*, 565.

Table 1. ^{1}H and $^{31}P\{^{1}H\}$ NMR parameters for compounds $MoOXY(PMe_3)_3$ (X, Y = Cl or I).

Compound	Solvent	$\delta_H(J_{HP}/Hz)$[a]	$\delta_P(J_{PP}/Hz)$
$MoOCl_2(PMe_3)_3$	acetone-d_6	1.68(d, 8.4) 1.63 (t, 3.9)	2.0 (t, 22) -5.2 (d, 22)
$MoOBr_2(PMe_3)_3$	acetone-d_6	1.73(d, 8.7) 1.73(t, 4.0)	-2.8 (t, 22) -9.4 (d, 22)
$MoOI_2(PMe_3)_3$	acetone-d_6	1.91(t, 4.0) 1.80(d, 8.7)	-12.5 (t, 20) -15.7 (d, 20)
$MoOI_2(PMe_3)_3$	C_6D_6	1.73 (t, 4.1) 1.36 (d, 8.4)	-14.98 (t, 22.2) -16.40 (d, 22.2)
$MoOClI(PMe_3)_3$, **A**[b]	acetone-d_6	1.71(d, 8.4) 1.80(t, 3.9)	2.2 (t, 20) -8.4 (d, 20)
$MoOClI(PMe_3)_3$, **B**[b]	acetone-d_6	n.i.[d] n.i.[d]	-9.7 (t, 20) -12.0 (d, 20)
$MoOBrI(PMe_3)_3$, **A'**[c]	acetone-d_6	1.84(t, 4.0) 1.74(d, 8.7)	-3.6 (t, 23) -11.0 (d, 23)
$MoOBrI(PMe_3)_3$, **B'**[c]	acetone-d_6	n.i.[d] n.i.[d]	-10.3 (t, 22) -13.8 (d, 22)

[a]vt = virtual triplet. [b]**A**: I *trans* to O; **B**: Cl *trans* to O (see Scheme 5). [c]**A'**: I *trans* to O; **B'**: Cl *trans* to O (see Scheme 6). [d]not identified.

Table 2. Selected bond distances (Å) and angles (°) for compound $MoOI_2(PMe_3)_3$.

Mo(1)-P(1)	2.4939(15)	Mo(1)-O(1)	1.685(4)
Mo(1)-P(2)	2.5073(14)	Mo(1)-I(1)	2.8634(6)
Mo(1)-P(3)	2.5130(15)	Mo(1)-I(2)	2.9207(6)
O(1)-Mo(1)-P(1)	82.16(15)	P(1)-Mo(1)-P(2)	93.80(5)
O(1)-Mo(1)-P(2)	99.94(15)	P(1)-Mo(1)-P(3)	92.38(5)
O(1)-Mo(1)-P(3)	102.79(15)	P(2)-Mo(1)-P(3)	157.06(5)
O(1)-Mo(1)-I(1)	93.43(15)	P(1)-Mo(1)-I(1)	175.50(4)
O(1)-Mo(1)-I(2)	172.20(15)	P(1)-Mo(1)-I(2)	90.08(4)
P(2)-Mo(1)-I(1)	87.84(4)	P(3)-Mo(1)-I(1)	87.70(4)
P(2)-Mo(1)-I(2)	79.76(3)	P(3)-Mo(1)-I(2)	78.16(4)
I(1)-Mo(1)-I(2)	94.343(17)		

Table 3. ATRP of styrene using $MoOX_2(PMe_3)_3$ (X = Cl, I) catalysts.[a]

Entry	X	Mo:I:Al:S[b]	k_{app}/min^{-1}
1	Cl	1:1:-:200	2.18E-04
2	Cl	1:1:1:200	4.38E-04
3	I	1:1:-:200	4.26E-04
4	I	1:1:1:200	9.54E-04

[a] All polymerizations were carried out in toluene at 90 ºC. [b]I = initiator (BEB); Al = $Al(O\textit{i}Pr)_3$ co-catalyst; S = styrene.

Table 4. Crystal data and structure refinement.

Compound	$MoOI_2(PMe_3)_3$	$[MoCl_2O(PMe_3)(OPMe_3)]_2O$
Empirical formula	$C_9H_{27}I_2MoOP_3$	$C_{12}H_{36}Cl_4Mo_2O_5P_4$
Formula weight	593.96	717.97
Temperature, K	180(2)	180(2) K
Wavelength, Å	0.71073	0.71073 Å
Crystal system	Orthorhombic	Monoclinic
Space group	P 2_1 2_1 2_1	P 2_1/c
a, Å	9.9624(8)	16.6058(18)
b, Å	10.6370(10)	11.8087(12)
c, Å	18.8084(19)	16.099(2)
β, °		113.384(11)
Volume, $Å^3$	1993.1(3)	2897.7(6)
Z	4	4
Density (calc.), Mg/m^3	1.979	1.646
μ, mm^{-1}	3.982	1.474
F(000)	1128	1440
Crystal size, mm^3	0.38 x 0.32 x 0.28	0.14 x 0.09 x 0.08
Theta range, °	2.17 to 26.09	2.85 to 26.37
Reflections collected	19690	21350
Unique refl. (R_{int})	3874 (0.0455)	5900 (0.0663)
Completeness to theta, %	98.1 (26.09°)	99.8 (26.37°)
Absorption correction	Semi-empirical	Semi-empirical
Max. and min. trans.	0.4148 and 0.2387	0.8737 and 0.8359
Refinement method	Full-matrix L.S. on F^2	Full-matrix L.S. on F^2
Data /restraints/parameters	3874 / 0 / 154	5900 / 0 / 256
Goodness-of-fit on F^2	1.087	0.782
Final R indices [I>2σ(I)]	R1= 0.0287, wR2= 0.0816	R1= 0.0379, wR2= 0.0554
R indices (all data)	R1= 0.0295, wR2 = 0.0822	R1= 0.0899, wR2= 0.0648
Absolute structure parameter	0.00(2)	
Residual density, $e.Å^{-3}$	0.951 and -1.437	0.557 and -0.470

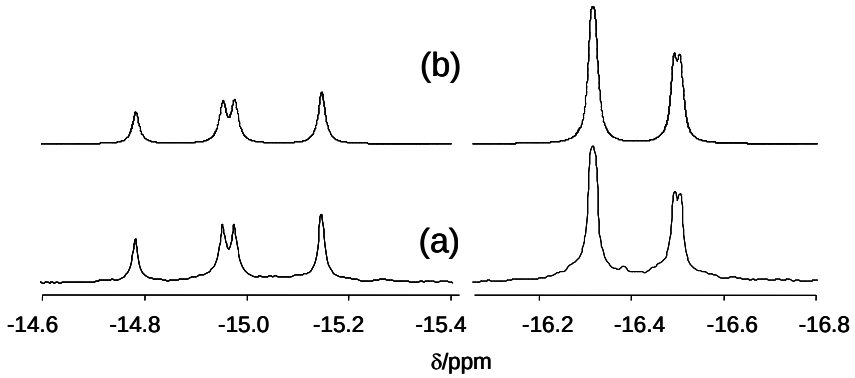

Figure 1. Experimental (a) and simulated (b) ^{31}P-NMR spectrum of compound $MoOI_2(PMe_3)_3$ in C_6D_6.

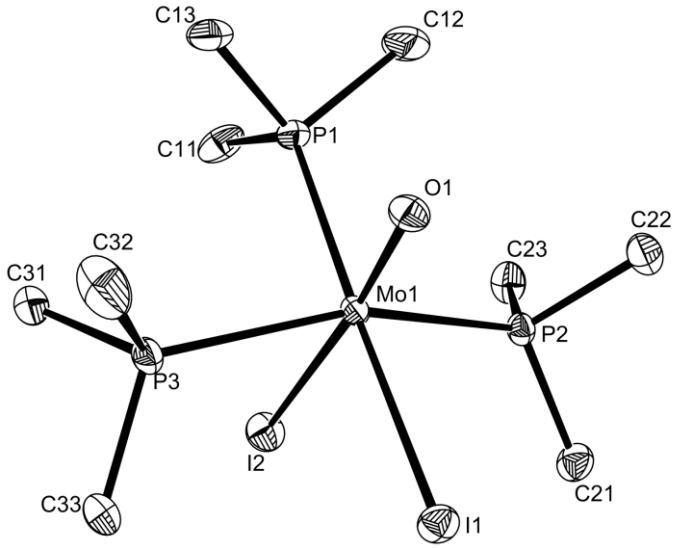

Figure 2. An ORTEP view of complex $MoOI_2(PMe_3)_3$. The ellipsoids are drawn at the 50% probability level.

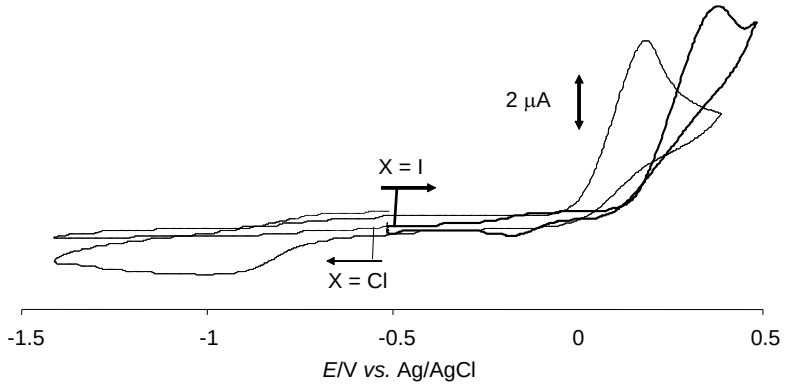

Figure 3. Cyclic voltammogram of compounds $MoOX_2(PMe_3)_3$ in THF. Thinner curve: X = Cl; thicker curve: X = I. $C_{Mo} = 4.10^{-3}$ M. Scan rate = 100 mV s^{-1}.

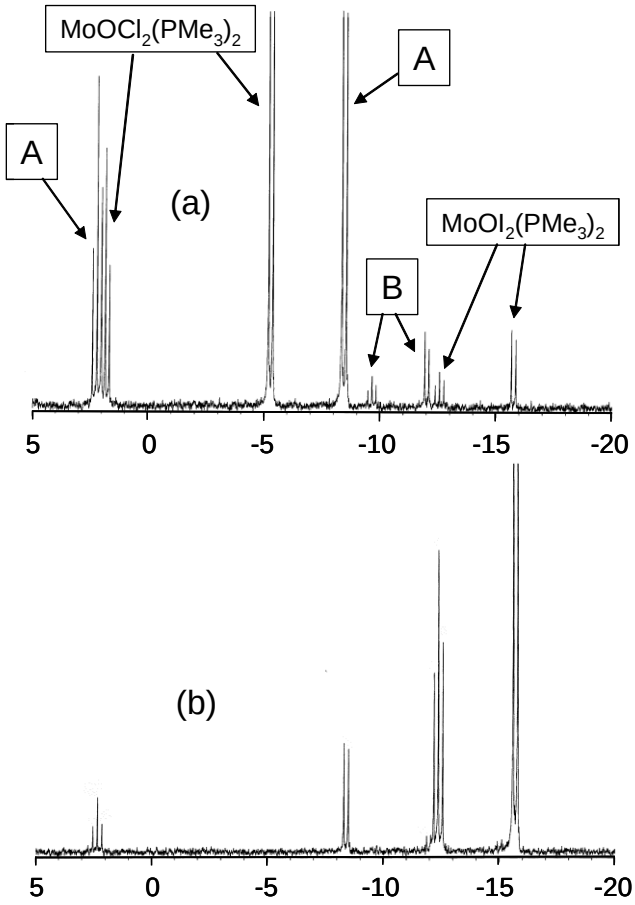

Figure 4. Room temperature $^{31}P\{^{1}H\}$ NMR spectra of $MoOCl_2(PMe_3)_3$ (50 mg, 0.12 mmol) and NaI in acetone-d_6 (0.6 mL). (a) After 5 h with 1 equiv NaI. (b) After 2.5 h from spectrum (a) with excess NaI.

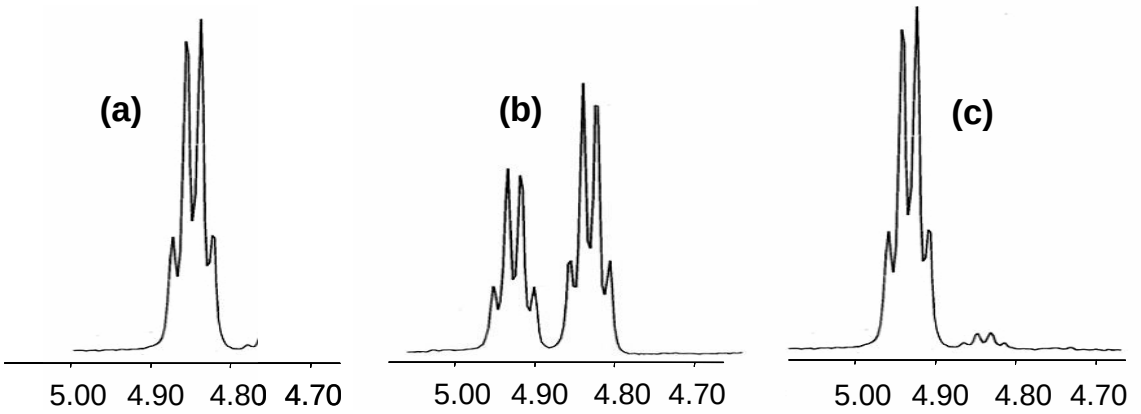

Figure 5. ^{1}H NMR monitoring of the halogen exchange between $MoOI_2(PMe_3)_3$ and BEB in toluene-d_8 at 90°C ([Mo] = [BEB] = ca. 0.1 mol l^{-1}). (a) t = 0. (b) t = 20 min. (c) t = 40 min.

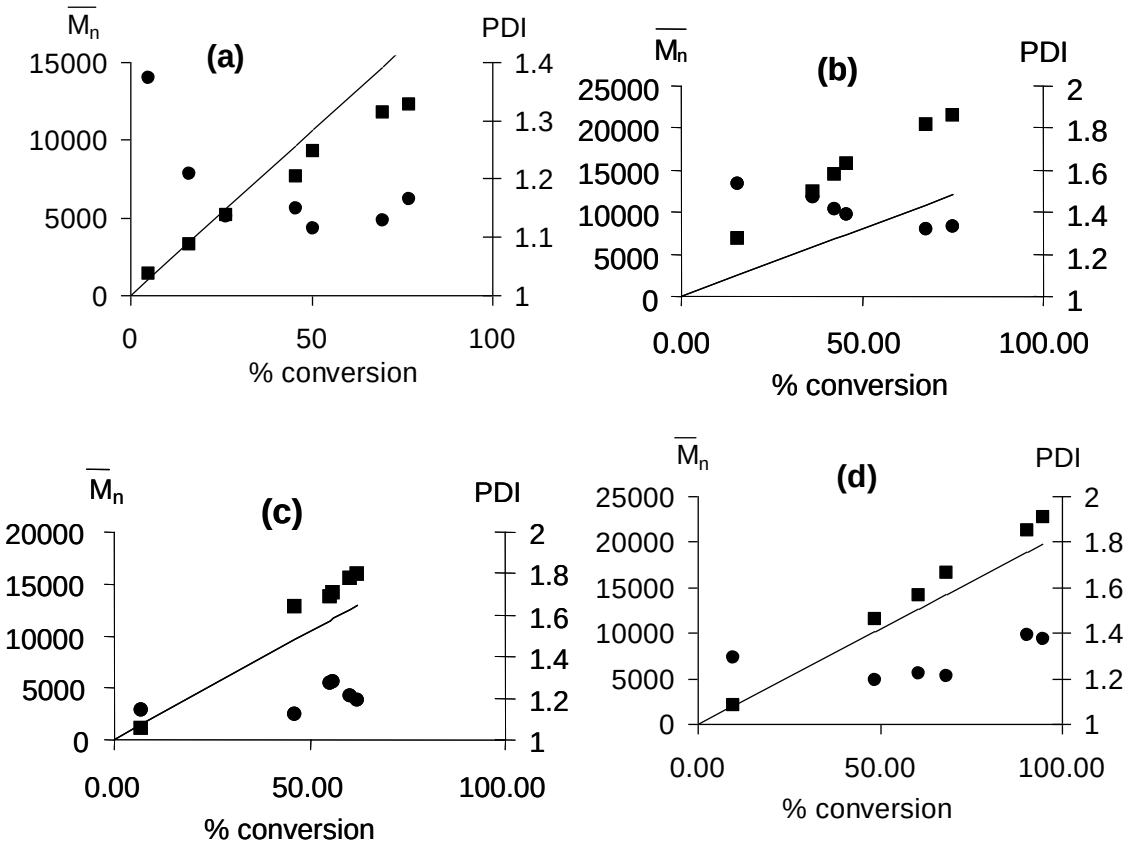

Figure 6. M_n vs. convertion and PDI for the ATRP of styrene catalyzed by $MoOX_2(PMe_3)_3$ (X = Cl, I). The conditions are given in Table 3 (entries 1-4). Squares: experimental M_n; circles: PDI; straight line: theoretical M_n. (a) X = Cl, no Al(O*i*Pr)$_3$ (entry 1); (b) X = Cl, with Al(O*i*Pr)$_3$ (entry 2); (c) X = I, no Al(O*i*Pr)$_3$ (entry 3); (d) X = I, with Al(O*i*Pr)$_3$ (entry 4).

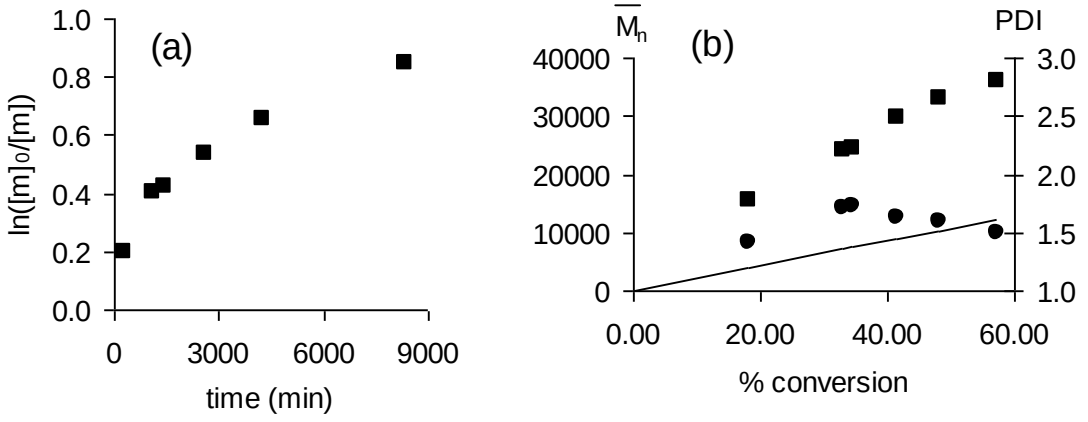

Figure 7. Polymerization of methyl acrylate catalyzed by $MoOCl_2(PMe_3)_3$ at 35°C. Conditions: Mo:I:Al:MA = 1:1:1:250 (MA = methyl acrylate; I (initiator) = ethyl 2-iodopropionate; Al = Al(O*i*Pr)$_3$). (a) Kinetics plot. (b) M_n vs. convertion and PDI for the Squares: experimental M_n; circles: PDI; straight line: theoretical M_n.

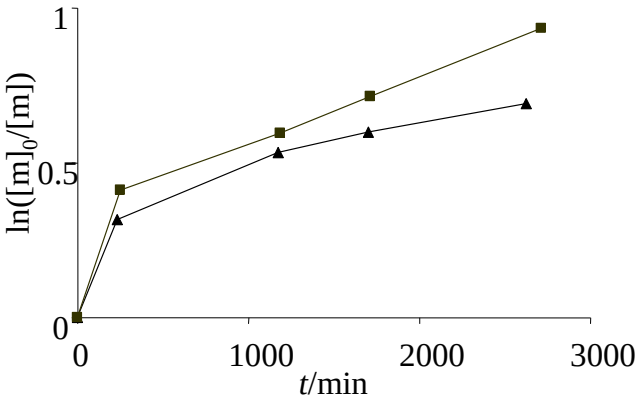

Figure 8. Polymerization of styrene in toluene (30% v/v) in the presence of the AIBN initiator (styrene/AIBN = 250) at 80°C. Squares: without Mo complex; triangles: with $MoOI_2(PMe_3)_3$ (AIBN/Mo = 1:1).

Scheme 1

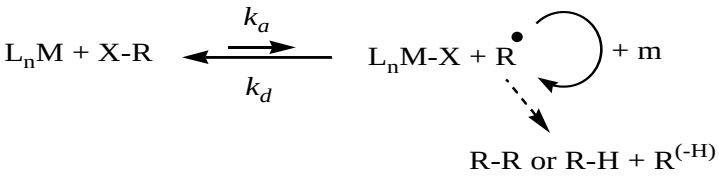

Scheme 2

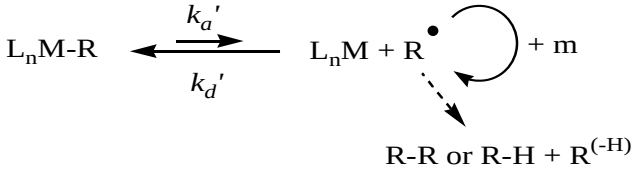

Scheme 3

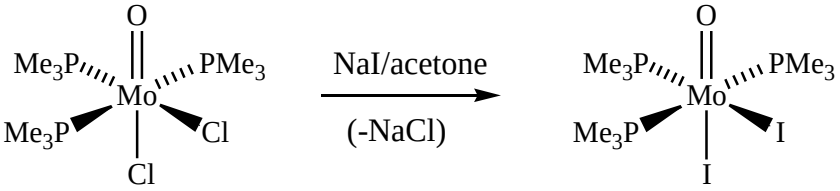

Scheme 4

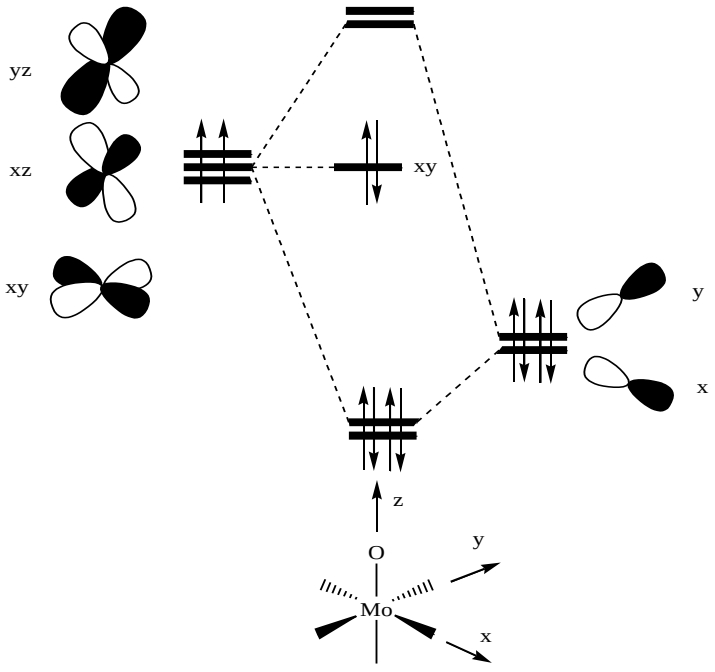

Scheme 5

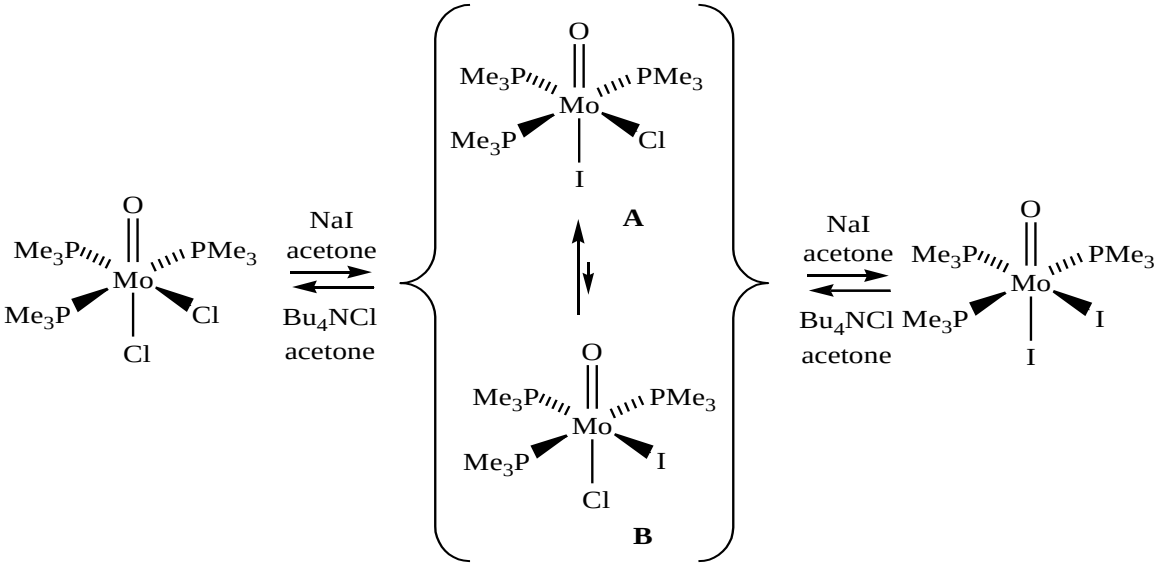

Scheme 6

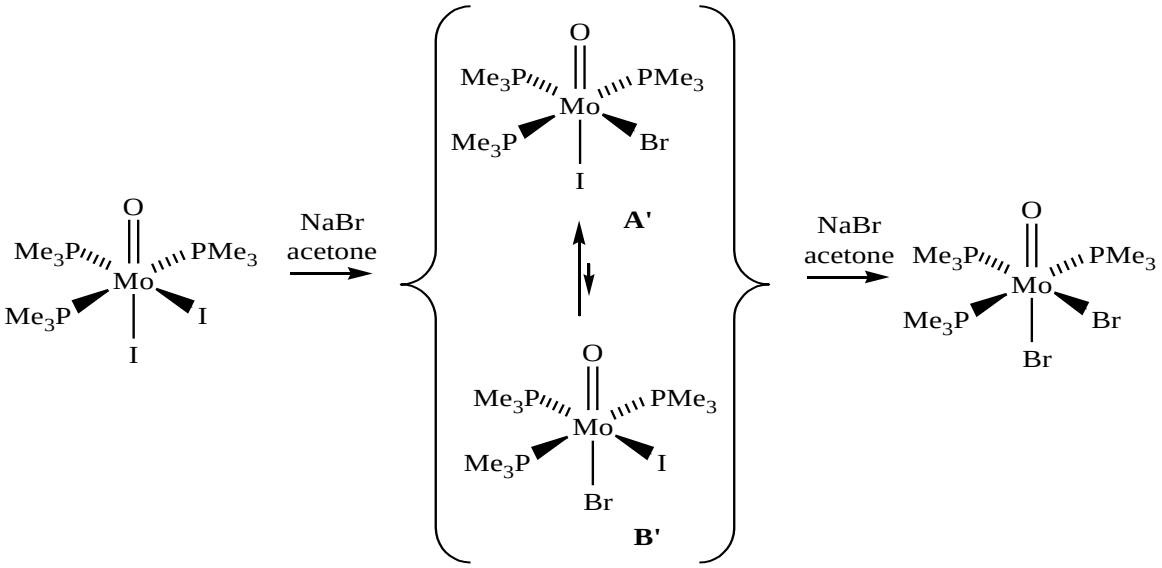

Scheme 7

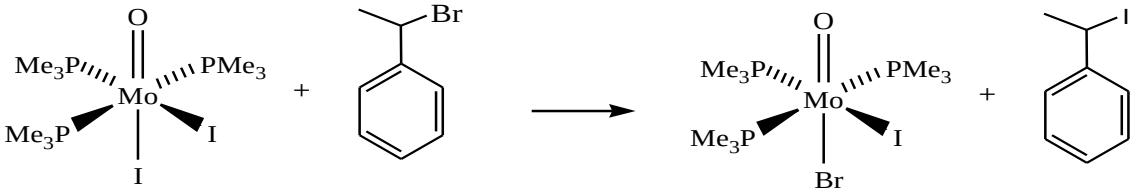
O
Me3P
PMe3
Mo
Me3P
I
I
+
Br
O
Me3P
PMe3
Mo
Me3P
I
Br
+
I

Graphical abstract